OUKA
The University of Osaka
Institutional Knowledge Archive

Title	Observation of intravalley spin scattering in a doped multivalley semiconductor
Author(s)	Hamaya, K.; Okada, T.; Kawashima, K. et al.
Citation	Physical Review B. 2025, 111(8), p. L081301
Version Type	VoR
URL	https://hdl.handle.net/11094/101980
rights	Copyright 2025 by the American Physical Society
Note	

The University of Osaka Institutional Knowledge Archive : OUKA

https://ir.library.osaka-u.ac.jp/

The University of Osaka

Letter

Observation of intravalley spin scattering in a doped multivalley semiconductor

K. Hamaya,[1,2,3,*] T. Okada,[3] K. Kawashima,[3] T. Naito,[3] K. Oki,[3] S. Kikuoka,[4] Y. Wagatsuma,[4] M. Yamada,[4] and K. Sawano[4]

[1]*Center for Spintronics Research Network, Graduate School of Engineering Science, Osaka University, 1-3 Machikaneyama, Toyonaka 560-8531, Japan*

[2]*Spintronics Research Network Division, Institute for Open and Transdisciplinary Research Initiatives, Osaka University, Suita, Osaka 565-0871, Japan*

[3]*Department of Systems Innovation, Graduate School of Engineering Science, Osaka University, 1-3 Machikaneyama, Toyonaka 560-8531, Japan*

[4]*Advanced Research Laboratories, Tokyo City University, 1-28-1 Tamazutsumi, Tokyo 158-8557, Japan*

(Received 24 September 2024; revised 22 January 2025; accepted 23 January 2025; published 18 February 2025)

To clarify spin-related phenomena within a single conduction valley of multivalley semiconductors, we experimentally study the effect of carrier concentration (n) on spin lifetime (τ_S) in strained $Si_{0.1}Ge_{0.9}$ at various temperatures. The spin diffusion length (λ) of strained $Si_{0.1}Ge_{0.9}$ is estimated from the contact distance dependence of the nonlocal spin signals for spin transport measurements in lateral spin-valve devices with varying n. The obtained λ is found to depend on n at temperatures below $\sim$100 K, with the estimated τ_S value at 8 K varying significantly with n, ranging from 0.2 to 6.2 ns. These features suggest the presence of intravalley spin scattering at low temperatures even in doped multivalley semiconductors. Thus, strained n-$Si_{0.1}Ge_{0.9}$ with L-valley energy splitting serves as a powerful tool for investigating the spin relaxation mechanisms in a single conduction valley of doped multivalley semiconductors.

DOI: 10.1103/PhysRevB.111.L081301

The study of spin relaxation mechanisms in semiconductors can effectively aid in the understanding of the physical phenomena in semiconductor spintronic devices [1–5]. For a III-V semiconductor GaAs, it is generally known that space inversion asymmetry in the zinc-blende crystal structure governs the spin relaxation in the doping conditions [D'yakonov-Perel' (DP) mechanism] [2,4,6–8]. For group-IV elements such as Si and Ge, on the other hand, space inversion symmetry can result in a negligibly small influence of the DP mechanism on spin relaxation [3,5,9,10]. Recently, possible spin-flip scattering processes between elliptical valleys (intervalley spin scattering) in the conduction bands of Si or Ge have been discussed in theoretical studies [11–17] and experimental ones [18–26].

In a past study [27], the spin lifetime for highly doped Si or Ge obtained by electron spin resonance measurements has been discussed in the context of the Elliott picture [11], indicating that intravalley spin-flip scattering was induced by the spin-orbit interaction in the host material, along with the momentum scattering of carriers. In the 2000s, theorists began reconsidering the Elliott-Yafet (EY) mechanism in Si and Ge [14,16,17]. In 2014, Song *et al.* theoretically proposed that the dominant spin relaxation in doped multivalley semiconductors, such as n-Si and n-Ge, is the intervalley spin-flip scattering induced by the central cell potential of impurities, referred to as donor-driven spin relaxation [17]. This is short-range spin scattering due to the spin-orbit coupling of the doped impurities, rather than the spin mixing of states due to the spin-orbit coupling in the host materials. Thus, the proposed theory differs from the simple Elliott process. Recent experimental studies demonstrated consistency with intervalley spin-flip scattering based on donor-driven spin relaxation in the low-temperature regime [22–26].

For Ge, the lattice strain dramatically changes the physical properties due to the energy proximity ($\sim$140 meV) between the conduction-band minima at L and Γ points. For example, tensile strain decreases the energy difference between the L and Γ gaps, thereby enhancing the optically accessible nature of Ge [28,29]. Even for spins, lifting the heavy-hole–light-hole degeneracy in the valence band of Ge leads to high spin polarization and long spin lifetime in strained Ge layers or Ge quantum wells grown on SiGe [30–33]. Recently, Naito *et al.* experimentally showed suppression of the impurity-induced intervalley spin-flip scattering at low temperatures using a strained n-$Si_{0.1}Ge_{0.9}$(111) layer [34]. In the study, the Ge-rich $Si_{1-x}Ge_x$ exhibited a Ge-like electronic band structure with conduction-band minima at the L points, while the in-plane and biaxial tensile strain in Ge-rich $Si_{1-x}Ge_x$(111) induced an energy splitting of the conduction L valleys [35,36]. However, the previous study was limited to using heavily doped layers with an impurity concentration (N_D) of 6.0×10^{18} cm^{-3} or 1.0×10^{19} cm^{-3} [34]. By intentionally controlling the N_D value down to $\sim 1.0 \times 10^{18}$ cm^{-3}, the influence of N_D or the carrier concentration (n) on the spin relaxation mechanism can be further investigated, even in a single conduction valley of the strained $Si_{0.1}Ge_{0.9}$.

In this Letter, we report on the significant impact of n on the spin lifetime (τ_S) of strained $Si_{0.1}Ge_{0.9}$ at various temperatures, using spin transport measurements in lateral spin-valve

*Contact author: hamaya.kohei.es@osaka-u.ac.jp

 ©2025 American Physical Society

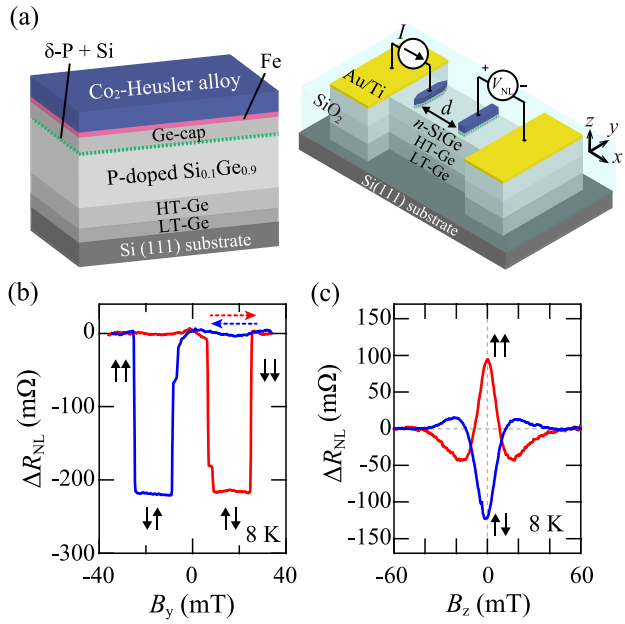

FIG. 1. (a) Schematics of a grown Co-based Heusler alloy/Fe/P δ-doped Ge/n-$Si_{0.1}Ge_{0.9}$ /Ge/Si(111) heterostructure (left) and a lateral spin-valve (LSV) device for spin transport measurements (right). (b) Nonlocal spin signal and (c) Hanle-effect curves for Device A with $d = 2.0$ μm and at 8 K.

(LSV) devices. We find that the spin diffusion length (λ) depends considerably on n below ∼100 K, with τ_S at 8 K varying significantly, ranging from 0.2 to 6.2 ns as n decreases from ∼7.0 × 10^{18} cm^{-3} to ∼7.0 × 10^{17} cm^{-3}. These features indicate the presence of intravalley spin scattering at low temperatures, even in doped multivalley semiconductors.

To examine the effects of N_D or n on τ_S at various temperatures, four-terminal nonlocal spin transport measurements were conducted in LSV devices with a semiconductor channel [2,22,24]. Coherently grown Ge-rich $Si_{1-x}Ge_x$ ($Si_{0.1}Ge_{0.9}$) spin transport layers with varying N_D values were used, fabricated on a Ge buffer layer atop a Si(111) substrate [34,37]. The heterostructure was grown using molecular beam epitaxy (MBE) as follows. First, a Ge (111) buffer layer on an undoped Si(111) substrate ($\rho \sim 1000\ \Omega$ cm) was formed using a two-step growth method [38], in which the first undoped Ge layer (∼30 nm) was grown at 350 °C (LT-Ge), followed by an undoped Ge layer (∼500 nm) grown at 700 °C (HT-Ge). The Ge buffer layer was relaxed, and the misfit dislocations were confined near the Ge/Si(111) interface, as shown in Ref. [34]. On the top of the HT-Ge layer, phosphorus (P)-doped n-$Si_{0.1}Ge_{0.9}$(111) layers were grown via MBE at 350 °C [39]. Finally, a 7-nm-thick P δ-doped Ge layer with a 0.3-nm-thick Si layer was grown on top of the spin transport layer for the Schottky tunnel conduction of electrons in spin transport measurements [10]. Co-based Heusler alloys, $Co_2FeAl_{0.5}Si_{0.5}$ and Co_2MnSi, grown on top of the Schottky tunnel barriers were used as the spin injector and detector [10,40–42]. The left side of Fig. 1(a) shows a schematic of the cross section of the Co-based Heusler alloy/n-$Si_{0.1}Ge_{0.9}$/Ge/Si(111) heterostructure grown via MBE. To enhance the spin signals, five or six Fe atomic layers were inserted between the Co-based Heusler alloy and n-$Si_{0.1}Ge_{0.9}$, as discussed in the literature [43,44].

Next, the LSV devices were fabricated. The right side of Fig. 1(a) illustrates the fabricated LSV device with a strained n-$Si_{0.1}Ge_{0.9}$ channel layer, where d is the edge-to-edge distance between the spin injector and detector. The size of the spin-injector (detector) contact was 0.4 × 5.0 μm^2 (1.0 × 5.0 μm^2). The details of the fabrication processes and top views of similar LSV devices have been reported in Ref. [10,45], where our LSV devices are not multiterminal spin injector devices. Table I compares the four LSV devices (A, B, C, and D) used in this study with various N_D values in the strained n-$Si_{0.1}Ge_{0.9}$ channel layer. To obtain the value of n, Hall bar devices were fabricated next to the LSV devices on the same $Si_{0.1}Ge_{0.9}$ layer. Also, to evaluate the value of λ, the various LSV devices with different d were designed as shown in Table I. Thus, the n dependence of λ and τ_S in strained n-$Si_{0.1}Ge_{0.9}$ was examined by changing the measurement temperature. All measurements were performed at various temperatures (8–298 K) by applying a negative direct current ($I < 0$), for which the spin-polarized electrons were injected into the channel used here by applying in-plane (B_y) or out-of-plane (B_z) magnetic fields.

Figure 1(b) shows a representative nonlocal spin signal [$\Delta R_{NL} = \Delta V_{NL}/I = (V_{NL}^{\uparrow\downarrow} - V_{NL}^{\uparrow\uparrow})/I$] as a function of B_y for Device A ($d = 2.0$ μm) at 8 K. The hysteretic behavior depending on the magnetization switching between the parallel and antiparallel states of the Co-based Heusler alloy electrodes is observed. As shown in Fig. 1(c), Hanle-type spin precession signals are also observed when B_z is applied under the parallel and antiparallel magnetization states. Although, in the Hanle curves in Fig. 1(c), background curves were subtracted from the raw data for clarity [2,10], the influences of the background curves were relatively great. Therefore, we did not conduct analyses with these Hanle curves. In any case, we note that these data mean that reliable spin transport in strained n-$Si_{0.1}Ge_{0.9}$ is observed experimentally in this study.

TABLE I. Impurity concentration (N_D), carrier concentration (n) at 298 and 8 K, electron mobility (μ) at 8 K, thickness (t_{SiGe}) and cross-sectional area (S_{SiGe}) of the strained $Si_{0.1}Ge_{0.9}$ channel, edge-edge contact distance (d), and ferromagnetic (FM) electrodes for various LSV devices.

	N_D (cm^{-3})	n at 298 K (cm^{-3})	n at 8 K (cm^{-3})	μ at 8 K (cm^2/V s)	t_{SiGe} (nm)	S_{SiGe} (μm^2)	d (μm)	FM electrodes
Device A	1.1×10^{18}	1.02×10^{18}	6.96×10^{17}	417	70	0.49	0.5,1.0,1.5,2.0	Co_2MnSi
Device B	2.0×10^{18}	1.17×10^{18}	1.63×10^{18}	564	140	0.98	1.0,1.5,2.0	Co_2MnSi
Device C	5.5×10^{18}	5.36×10^{18}	4.25×10^{18}	539	80	0.56	0.5,1.0,1.5,2.0	$Co_2FeAl_{0.5}Si_{0.5}$
Device D	1.2×10^{19}	1.04×10^{19}	7.14×10^{18}	404	70	0.49	0.5,1.0,1.5,2.0	Co_2MnSi

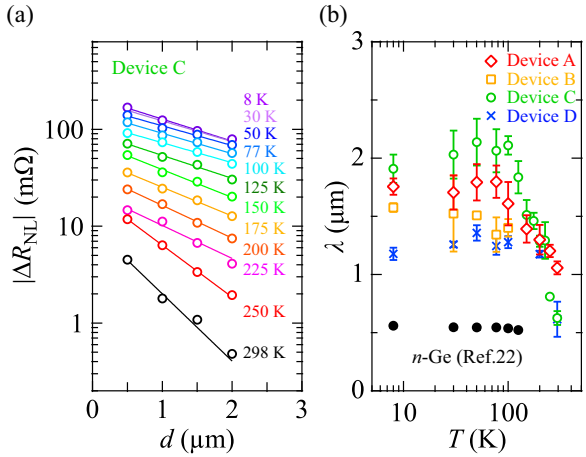

FIG. 2. (a) d dependence of $|\Delta R_{NL}|$ for Device C at various temperatures. The solid lines are fitted to Eq. (1). (b) T dependence of λ for all the LSV devices, together with that for the LSV with heavily doped Ge (black), reported in Ref. [22].

To determine λ in the strained n-$Si_{0.1}Ge_{0.9}$, ΔR_{NL} is measured for all the LSV devices with various d values at different temperatures. Figure 2(a) shows the d dependence of the magnitude of ΔR_{NL} ($|\Delta R_{NL}|$) for Device C at various temperatures. With increasing d, $|\Delta R_{NL}|$ decays exponentially at all investigated temperatures. In general, the decay of $|\Delta R_{NL}|$ with increasing d is expressed by the following equation [46–49]:

$$|\Delta R_{NL}| = P^2 \frac{\rho\lambda}{S} \exp(-d/\lambda), \tag{1}$$

where P is the average of the spin injection and detection efficiencies, and S is the cross-sectional area of the semiconductor channels (S_{SiGe} in Table I). The λ value can be estimated by fitting the decay of $|\Delta R_{NL}|$ into Eq. (1) in the T range of 8–298 K, as shown by the solid curves in Fig. 2(a). From these estimations, the T dependence of λ for all devices is presented in Fig. 2(b), together with our previously reported λ for n-Ge with n of $\sim 1.0 \times 10^{19}$ cm^{-3} [22]. We evidently observe relative enhancements in λ for all the devices with the strained n-$Si_{0.1}Ge_{0.9}$ compared with n-Ge in the low-temperature regime. This implies that the energy splitting of the conduction L valleys enables the suppression of intervalley spin-flip scattering at low temperatures [34]. Notably, clear variations are observed in λ with n in the strained n-$Si_{0.1}Ge_{0.9}$. Here, we infer that the energy-splitting values of the conduction L valleys are almost the same (∼90 meV) [35]. Nevertheless, the magnitude of the spin-flip scattering appears to vary by changing n in the strained n-$Si_{0.1}Ge_{0.9}$.

To further investigate the marked variation in λ even at low temperatures, we estimate τ_S using the relation $\lambda = \sqrt{D\tau_S}$ and the λ values in Fig. 2(b), where D is the diffusion constant. In this study, the value of D is determined using the modified Einstein relation in Eq. (4) in Ref. [50], and the values of n and μ are experimentally obtained by the transport measurements with Hall bar devices. Figures 3(a) and 3(b) show the T dependent τ_S and D, respectively, for all devices with strained n-$Si_{0.1}Ge_{0.9}$ (various n). An evident variation in τ_S is observed when T is reduced to less than ∼100 K. Notably,

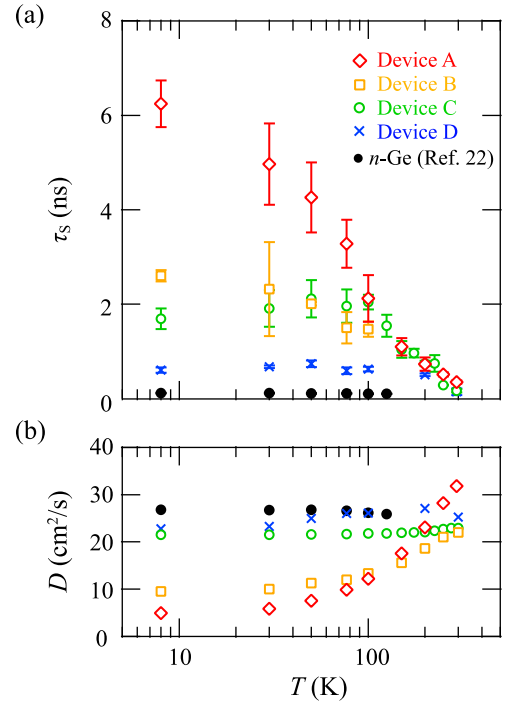

FIG. 3. Temperature dependence of (a) τ_S and (b) D for all devices, along with previously reported values for n-Ge from Ref. [22].

the value of τ_S for Device A significantly increases with decreasing temperature, whereas for Device D, it is nearly constant from 8 to 200 K, similar to the case of LSVs with a heavily doped Ge channel [22]. At 8 K, the τ_S value is found to widely modulate from 0.2 to 6.2 ns for n varying from $\sim 7.14 \times 10^{18}$ cm^{-3} to $\sim 6.96 \times 10^{17}$ cm^{-3}, respectively. These features cannot be understood solely by the suppression of intervalley spin-flip scattering due to the energy splitting of the conduction L valleys in strained n-$Si_{0.1}Ge_{0.9}$.

To gain insights on the above significant n dependence on τ_S, f_S/f_P versus n is plotted for all devices at various temperatures, as shown in Fig. 4(a), where f_S and f_P denote

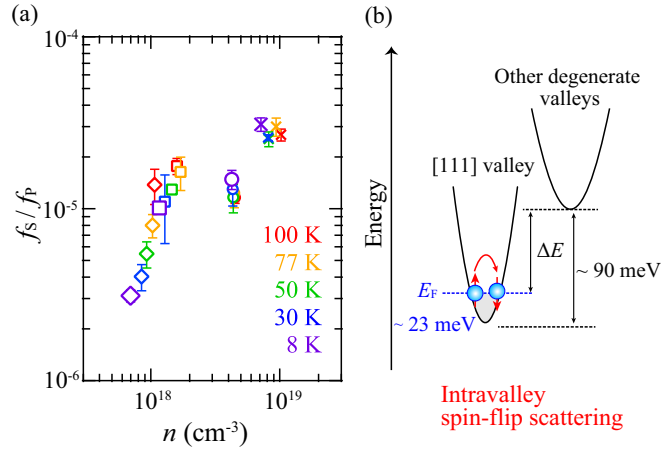

FIG. 4. (a) f_S/f_P as a function of n at various temperatures. (b) Schematic of the intravalley spin-flip scattering in a single conduction-band valley of the strained n-$Si_{0.1}Ge_{0.9}$ with $n = 1.0 \times 10^{18}$ cm^{-3} at 8 K.

the spin-scattering and momentum-scattering frequencies, respectively, estimated from $\frac{1}{\tau_S}$ and $\frac{1}{\tau_P}$. The value of τ_P is estimated from the relation $\tau_P = m^*\mu/q$, where m^*, μ, and q are the effective masses of the conduction electrons in the lower valley ($0.082\,m_0$) [51], electron mobility, and elemental charge, respectively. Figure 4(a) shows that the values of f_S/f_P at low temperatures are less than 10^{-4}, indicating that fewer than one spin-flip scattering occurs during the 10^4 times momentum scattering. Markedly small values of f_S/f_P were also reported for the Si two-dimensional inversion layer at low temperatures [52]. Notably, even at the same temperature, for example 8 K, the values of f_S/f_P vary significantly with changing n. These features indicate the presence of another spin-scattering mechanism that depends on n at low temperatures in a single conduction valley of strained n-$Si_{0.1}Ge_{0.9}$.

A possible spin-scattering mechanism that depends on n at low temperatures in strained n-$Si_{0.1}Ge_{0.9}$ is shown in Fig. 4(b). The Fermi level (E_F) above the conduction-band edge can be roughly estimated as $\hbar^2(3\pi^2 n)^{2/3}/(2m_e)$ ($\sim$23 meV for $n = 1.0 \times 10^{18}$ cm^{-3} at 8 K), and the valley energy splitting ($\sim$90 meV) after applying a biaxial tensile strain in (111) to a Ge-like conduction band is also shown [35,36]. In this case, intervalley spin-flip scattering is fully suppressed because of a sufficiently large energy splitting (ΔE). Here, because the value of f_S/f_P reaches less than 10^{-5} at low temperatures for $n \lesssim 1.0 \times 10^{18}$ cm^{-3}, it can be inferred that almost no spin scattering occurs via momentum scattering of electrons. However, with increasing n, the value of f_S/f_P is slightly enhanced, even at 8 K. This variation in f_S/f_P implies the presence of another mechanism, that is, intravalley spin-flip scattering in the lower valley, as illustrated in Fig. 4(b).

Finally, we discuss origins of the intravalley spin-flip scattering in the lower valley of the strained n-$Si_{0.1}Ge_{0.9}$. As one of the origins, we can consider the influence of the doped impurity (phosphorus). Because the value of n indicates the concentration of the ionized doped impurity, it is possible that a donor-driven intravalley spin-flip scattering begins to influence the spin relaxation mechanism [17], even in a single conduction valley of the strained n-$Si_{0.1}Ge_{0.9}$. Another is the possibility for the existence of the DP mechanism even in the strained n-$Si_{0.1}Ge_{0.9}$. The temperature-dependent and n-dependent τ_S, shown in Fig. 3(a), are similar to those for the DP mechanism in n-GaAs discussed in Refs. [7,8]. If there is broken inversion symmetry in the strained n-$Si_{0.1}Ge_{0.9}$ channel in our LSV devices, one can believe the presence of the spin-orbit field due to the DP mechanism. Having eliminated the intervalley spin-flip scattering at low temperatures, one can infer that they could reach a relatively long spin lifetime, originating from a DP-like spin relaxation process [7,8]. Namely, the DP spin relaxation mechanism may also be an origin of the intravalley spin scattering mechanism in the strained n-$Si_{0.1}Ge_{0.9}$. From these considerations, the spin relaxation phenomenon observed here in a single valley is different from the intravalley spin-flip scattering based on the simple Elliott picture described in the introduction [27]. It is generally difficult to detect these features in degenerate conduction valleys in Si and Ge. In future, the related phenomena will be focused in the field of SiGe optical and quantum information technologies [53,54].

In summary, significant effects of n were observed on the spin lifetime at low temperatures in strained $Si_{0.1}Ge_{0.9}$. This can be interpreted in terms of the presence of intravalley spin scattering, different from that based on a simple Elliott picture. Strained n-$Si_{0.1}Ge_{0.9}$(111) with L-valley energy splitting is a powerful tool for studying the spin relaxation mechanism in a single conduction valley of doped multivalley semiconductors.

This work was supported in part by JSPS KAKENHI (Grants No. 19H05616, No. 21H05000, and No. 24H00034), JST-ASPIRE (Grant No. JPMJAP2413), and MEXT X-NICS (Grant No. JPJ011438), and Spintronics Research Network of Japan (Spin-RNJ).

[1] I. Žutić, J. Fabian, and S. D. Sarma, Spintronics: Fundamentals and applications, Rev. Mod. Phys. **76**, 323 (2004).

[2] X. Lou, C. Adelmann, S. A. Crooker, E. S. Garlid, J. Zhang, K. S. M. Reddy, S. D. Flexner, C. J. Palmstrøm, and P. A. Crowell, Electrical detection of spin transport in lateral ferromagnet–semiconductor devices, Nat. Phys. **3**, 197 (2007).

[3] I. Appelbaum, B. Huang, and D. J. Monsma, Electronic measurement and control of spin transport in silicon, Nature (London) **447**, 295 (2007).

[4] M. Ciorga, A. Einwanger, U. Wurstbauer, D. Schuh, W. Wegscheider, and D. Weiss, Electrical spin injection and detection in lateral all-semiconductor devices, Phys. Rev. B **79**, 165321 (2009).

[5] T. Sasaki, T. Oikawa, T. Suzuki, M. Shiraishi, Y. Suzuki, and K. Noguchi, Temperature dependence of spin diffusion length in silicon by Hanle-type spin precession, Appl. Phys. Lett. **96**, 122101 (2010).

[6] M. I. D'yakonov and V. I. Perel', Spin relaxation of conduction electrons in noncentrosymmetric semiconductors, Sov. Phys. Solid State **13**, 3023 (1972).

[7] R. I. Dzhioev, K. V. Kavokin, V. L. Korenev, M. V. Lazarev, B. Ya. Meltser, M. N. Stepanova, B. P. Zakharchenya, D. Gammon, and D. S. Katzer, Low-temperature spin relaxation in n-type GaAs, Phys. Rev. B **66**, 245204 (2002).

[8] T. A. Peterson, S. J. Patel, C. C. Geppert, K. D. Christie, A. Rath, D. Pennachio, M. E. Flatté, P. M. Voyles, C. J. Palmstrøm, and P. A. Crowell, Spin injection and detection up to room temperature in Heusler alloy/n-GaAs spin valves, Phys. Rev. B **94**, 235309 (2016).

[9] R. Jansen, Silicon spintronics, Nat. Mater. **11**, 400 (2012).

[10] K. Hamaya, Y. Fujita, M. Yamada, M. Kawano, S. Yamada, and K. Sawano, Spin transport and relaxation in germanium, J. Phys. D **51**, 393001 (2018).

[11] R. J. Elliott, Theory of the effect of spin-orbit coupling on magnetic resonance in some semiconductors, Phys. Rev. **96**, 266 (1954).

[12] Y. Yafet, in *Solid State Physics*, edited by F. Seitz and D. Turnbull (Academic, New York, 1963), Vol. 14.

[13] P. Li and H. Dery, Spin-orbit symmetries of conduction electrons in silicon, Phys. Rev. Lett. **107**, 107203 (2011).

[14] J-M. Tang, B. T. Collins, and M. E. Flatté, Electron spin-phonon interaction symmetries and tunable spin relaxation in silicon and germanium, Phys. Rev. B **85**, 045202 (2012).

[15] Y. Song and H. Dery, Analysis of phonon-induced spin relaxation processes in silicon, Phys. Rev. B **86**, 085201 (2012).

[16] P. Li, Y. Song, and H. Dery, Intrinsic spin lifetime of conduction electrons in germanium, Phys. Rev. B **86**, 085202 (2012).

[17] Y. Song, O. Chalaev, and H. Dery, Donor-driven spin relaxation in multivalley semiconductors, Phys. Rev. Lett. **113**, 167201 (2014).

[18] C. Guite and V. Venkataraman, Measurement of electron spin lifetime and optical orientation efficiency in germanium using electrical detection of radio frequency modulated spin polarization, Phys. Rev. Lett. **107**, 166603 (2011).

[19] C. Guite and V. Venkataraman, Temperature dependence of spin lifetime of conduction electrons in bulk germanium, Appl. Phys. Lett. **101**, 252404 (2012).

[20] P. Li, J. Li, L. Qing, H. Dery, and I. Appelbaum, Anisotropy-driven spin relaxation in germanium, Phys. Rev. Lett. **111**, 257204 (2013).

[21] A. Giorgioni, E. Vitiello, E. Grilli, M. Guzzi, and F. Pezzoli, Valley-dependent spin polarization and long-lived electron spins in germanium, Appl. Phys. Lett. **105**, 152404 (2014).

[22] Y. Fujita, M. Yamada, S. Yamada, T. Kanashima, K. Sawano, and K. Hamaya, Temperature-independent spin relaxation in heavily doped n-type germanium, Phys. Rev. B **94**, 245302 (2016).

[23] Y. Fujita, M. Yamada, M. Tsukahara, T. Oka, S. Yamada, T. Kanashima, K. Sawano, and K. Hamaya, Spin transport and relaxation up to 250 K in heavily doped n-type ge detected using $Co_2FeAl_{0.5}Si_{0.5}$ Electrodes, Phys. Rev. Appl. **8**, 014007 (2017).

[24] M. Ishikawa, T. Oka, Y. Fujita, H. Sugiyama, Y. Saito, and K. Hamaya, Spin relaxation through lateral spin transport in heavily doped n-type silicon, Phys. Rev. B **95**, 115302 (2017).

[25] M. Yamada, Y. Fujita, M. Tsukahara, S. Yamada, K. Sawano, and K. Hamaya, Large impact of impurity concentration on spin transport in degenerate n-Ge, Phys. Rev. B **95**, 161304(R) (2017).

[26] M. Yamada, T. Ueno, T. Naito, K. Sawano, and K. Hamaya, Experimental extraction of donor-driven spin relaxation in n-type nondegenerate germanium, Phys. Rev. B **104**, 115301 (2021).

[27] E. M. Gershenzon, N. M. Pevin, and M. S. Fogelson, Spin relaxation of conduction electrons in highly doped semiconductors (InSb, Si, Ge), Phys. Status Solidi B **49**, 287 (1972).

[28] J. Liu, X. Sun, D. Pan, X. Wang, L. C. Kimerling, T. L. Koch, and J. Michel, Tensile-strained, n-type Ge as a gain medium for monolithic laser integration on Si, Opt. Express **15**, 11272 (2007).

[29] J. Michel, J. Liu, and L. C. Kimerling, High-performance Ge-on-Si photodetectors, Nat. Photon. **4**, 527 (2010).

[30] F. Bottegoni, G. Isella, S. Cecchi, and F. Ciccacci, Spin polarized photoemission from strained Ge epilayers, Appl. Phys. Lett. **98**, 242107 (2011).

[31] F. Pezzoli, F. Bottegoni, D. Trivedi, F. Ciccacci, A. Giorgioni, P. Li, S. Cecchi, E. Grilli, Y. Song, M. Guzzi, H. Dery, and G. Isella, Optical spin injection and spin lifetime in Ge heterostructures, Phys. Rev. Lett. **108**, 156603 (2012).

[32] E. Vitiello, M. Virgilio, A. Giorgioni, J. Frigerio, E. Gatti, S. De Cesari, E. Bonera, E. Grilli, G. Isella, and F. Pezzoli, Spin-dependent direct gap emission in tensile-strained Ge films on Si substrates, Phys. Rev. B **92**, 201203(R) (2015).

[33] N. W. Hendrickx, W. I. L. Lawrie, L. Petit, A. Sammak, G. Scappucci, and M. Veldhorst, A single-hole spin qubit, Nat. Commun. **11**, 3478 (2020).

[34] T. Naito, M. Yamada, S. Yamada, K. Sawano, and K. Hamaya, Suppression of donor-driven spin relaxation in strained $Si_{0.1}Ge_{0.9}$, Phys. Rev. Appl. **13**, 054025 (2020).

[35] Q. M. Ma and K. L. Wang, Strain-induced nonlinear energy–band splitting of $Si_{1-x}Ge_x$ alloys coherently grown on (111) and (110) oriented Ge substrates, Appl. Phys. Lett. **58**, 1184 (1991).

[36] R. Vrijen, E. Yablonovitch, K. Wang, H. W. Jiang, A. Balandin, V. Roychowdhury, T. Mor, and D. DiVincenzo, Electron-spin-resonance transistors for quantum computing in silicon-germanium heterostructures, Phys. Rev. A **62**, 012306 (2000).

[37] T. Naito, M. Yamada, Y. Wagatsuma, K. Sawano, and K. Hamaya, Effect of strain on room-temperature spin transport in $Si_{0.1}Ge_{0.9}$, Phys. Rev. Appl. **18**, 024005 (2022).

[38] K. Sawano, Y. Hoshi, S. Kubo, K. Arimoto, J. Yamanaka, K. Nakagawa, K. Hamaya, M. Miyao, and Y. Shiraki, Structural and electrical properties of Ge(111) films grown on Si(111) substrates and application to Ge(111)-on-Insulator, Thin Solid Films **613**, 24 (2016).

[39] Y. Wagatsuma, M. M. Alam, K. Okada, M. Yamada, K. Hamaya, and K. Sawano, A drastic increase in critical thickness for strained SiGe by growth on mesa-patterned Ge-on-Si, Appl. Phys. Express **14**, 025502 (2021).

[40] Y. Sakuraba, M. Hattori, M. Oogane, Y. Ando, H. Kato, A. Sakuma, T. Miyazaki, and H. Kubota, Giant tunneling magnetoresistance in $Co_2MnSi/Al-O/Co_2MnSi$ magnetic tunnel junctions, Appl. Phys. Lett. **88**, 192508 (2006).

[41] P. Bruski, Y. Manzke, R. Farshchi, O. Brandt, J. Herfort, and M. Ramsteiner, All-electrical spin injection and detection in the Co_2FeSi/GaAs hybrid system in the local and non-local configuration, Appl. Phys. Lett. **103**, 052406 (2013).

[42] K. Hamaya and M. Yamada, Semiconductor spintronics with Co_2-Heusler compounds, MRS Bull. **47**, 584 (2022).

[43] M. Yamada, F. Kuroda, M. Tsukahara, S. Yamada, T. Fukushima, K. Sawano, T. Oguchi, and K. Hamaya, Spin injection through energy-band symmetry matching with high spin polarization in atomically controlled ferromagnet/ferromagnet/semiconductor structures, NPG Asia Mater. **12**, 47 (2020).

[44] K. Kudo, M. Yamada, S. Honda, Y. Wagatsuma, S. Yamada, K. Sawano, and K. Hamaya, Room-temperature two-terminal magnetoresistance ratio reaching 0.1% in semiconductor-based lateral devices with $L2_1$-ordered Co_2MnSi, Appl. Phys. Lett. **118**, 162404 (2021).

[45] Y. Fujita, M. Yamada, M. Tsukahara, T. Naito, S. Yamada, K. Sawano, and K. Hamaya, Nonmonotonic bias dependence of local spin accumulation signals in ferromagnet/semiconductor lateral spin-valve devices, Phys. Rev. B **100**, 024431 (2019).

[46] M. Johnson and R. H. Silsbee, Interfacial charge-spin coupling: Injection and detection of spin magnetization in metals, Phys. Rev. Lett. **55**, 1790 (1985).

[47] F. J. Jedema, H. B. Heersche, A. T. Filip, J. J. A. Baselmans, and B. J. van Wees, Electrical detection of spin precession in a metallic mesoscopic spin valve, Nature (London) **416**, 713 (2002).

[48] T. Kimura and Y. Otani, Spin transport in lateral ferromagnetic/nonmagnetic hybrid structures, J. Phys.: Condens. Matter **19**, 165216 (2007).

[49] T. Kimura, N. Hashimoto, S. Yamada, M. Miyao, and K. Hamaya, Room-temperature generation of giant pure spin currents using epitaxial Co_2FeSi spin injectors, NPG Asia Mater. **4**, e9 (2012).

[50] M. E. Flatté and J. M. Byers, Spin Diffusion in Semiconductors, Phys. Rev. Lett. **84**, 4220 (2000).

[51] W. G. Spitzer, F. A. Trumbore, and R. A. Logan, Properties of heavily doped n-type germanium, J. Appl. Phys. **32**, 1822 (1961).

[52] S. Sato, M. Tanaka, and R. Nakane, Electron spin transport in a metal-oxide-semiconductor Si two-dimensional inversion channel: Effect of hydrogen annealing on spin-scattering mechanism and spin lifetime, Phys. Rev. Appl. **18**, 064071 (2022).

[53] M. Bonfanti, E. Grilli, and M. Guzzi, M. Virgilio and G. Grosso, D. Chrastina, G. Isella, H. von Känel, and A. Neels, Optical transitions in Ge/SiGe multiple quantum wells with Ge-rich barriers, Phys. Rev. B **78**, 041407(R) (2008).

[54] T.-K. Hsiao, P. Cova Fariña, S. D. Oosterhout, D. Jirovec, X. Zhang, C. J. van Diepen, W. I. L. Lawrie, C.-A. Wang, A. Sammak, G. Scappucci, M. Veldhorst, E. Demler, and L. M. K. Vandersypen, Exciton transport in a germanium quantum dot ladder, Phys. Rev. X **14**, 011048 (2024).